RZ 3283 (# 93329) 10/30/00
Mathematics & Physics 15 pages

Research Report

Charge-carrier injection into polymorphic forms of CuPc: A scanning tunneling microscopy study

L. Rossi, P. Müller, S.F. Alvarado, and W. Riess

IBM Research
Zurich Research Laboratory
8803 Rüschlikon
Switzerland

Charge-carrier injection into polymorphic forms of CuPc: A scanning tunneling microscopy study

L. Rossi, P. Müller, S.F. Alvarado, and W. Riess

IBM Research, Zurich Research Laboratory, 8803 Rüschlikon, Switzerland

Abstract

In this work injection of charge carriers into the empty and filled states of copper phthalocyanine (CuPc) thin films is investigated by scanning tunneling microscopy and spectroscopy. Measurements of the threshold energy for electrons and holes from the tip of the scanning electron microscope allows us to determine the so-called single-particle band gap (E_{gsp}) of different polymorphic phases present on CuPc thin films. We find that the value of E_{gsp} depends on the crystal structure and packing density of the material, E_{gsp} being in the range of 0.18 to 1.1 eV, which is much smaller than the optical band gap of $\sim$1.7 eV. The lowest values of E_{gsp} are found for the crystalline phases of CuPc, obtained by thermal annealing, whereas the largest values and inferior charge-transport properties are found for unannealed samples where the packing density of the CuPc molecules and long-range crystallographic order appear to be lowest. This discrepancy indicates the presence of intermolecular interactions giving rise to "in-gap" states that can play a predominant role in controlling injection as well as transport properties of charge carriers into this material relevant, for applications in organic electroluminescent devices for example.

I. INTRODUCTION

Copper phthalocyanine (CuPc) is a very well-known dye pigment with a number of interesting properties, e.g. it is an organic semiconductor, it is chemically and thermally very stable, it can easily form ordered thin films, and it shows photoconductivity and is used for catalysis. Lately, it has been studied for electronic and photonic device applications, in particular for organic light-emitting devices (OLEDs) [1–3]. It has been shown that a CuPc layer, inserted between the anode (typically indium-tin-oxide (ITO) on glass) and the hole-transport layer (HTL) of an OLED structure [2,3], produces a significant improvement in device-lifetime by preventing interface degradation at the HTL/ITO interface, and additionally, stabilizing the hole-injection barrier [4]. Recently, CuPc has also been used as a buffer layer in transparent cathodes [5,6], where it does not seem to impede electron transport [6]. Despite this technical progress the comprehension of the basic mechanisms underlying charge injection and transport in CuPc is still very limited. To our knowledge some fundamental issues that have not yet been addressed are related to the effect the different polymorphic phases on charge-carrier injection and transport. For example the charge carrier mobility of a given material as well as the barrier height at the interfaces between thin layers in a device can be strongly influenced by the molecular order and packing density. In particular, an accurate picture of both the effect of intermolecular interactions on the electronic structure of bulk materials and the energy level alignment at different interfaces in an OLED is still missing. Recently, the effect of crystallization on the performance of OLEDs was studied by Gao et al. who find that high-temperature processing to induce crystallization of the hole transport layer leads to a substantial increase in luminescent efficiency and brightness of OLEDs [7]. This result contradicts the common belief that crystallization of the organic layers leads to the degradation of OLEDs.

In the present work we investigate the influence of crystallinity and the packing density of CuPc on the electronic level energy of the lowest unoccupied and the highest occupied molecular orbitals (LUMO and HOMO respectively) involved in charge injection and transport. Up to now, several tunneling spectroscopy studies have been performed on monolayer or submonolayer thin films [8–11], whereas the effect of additional layers on the electronic properties has been disregarded. This effect can be important because nonresonant tunneling through a single molecule to the substrate is not negligible. In addition, interactions with the substrate can influence the electronic properties. For instance the spacing between the electronic levels of single molecules in contact with the substrate can be different than for a molecule in the bulk of the material. For multilayer coverage, however, charge injection and transport is mediated by bulk states. Here we present results that allow us to determine the height of the energy barrier for the injection of electrons and holes as well as the charge-injection gap for various CuPc polymorphic phases on films approximately 10 nm thick, i.e. approximately 30-40 monolayers.

II. EXPERIMENTAL

CuPc thin films were deposited by sublimation on a Au(111) single crystal surface under ultrahigh vacuum (UHV) conditions (base pressure in the lower 10^{-10} mbar range). The Au(111) single crystal was cleaned by several cycles of Ne-ion bombardment at kinetic energies of 600 to 800 eV, and annealed at temperatures up to 360°C for 8 h. STM imaging reveals atomically flat crystal terraces several 100 nm wide and the typical herringbone reconstruction of the Au(111) surface [12]. The Au(111) step height between neighboring monoatomic terraces

was used to calibrate the z motion of the piezoscanner. The temperature of the resistively heated sublimation source was approximately 380°C for a growth rate of 0.33 nm/s, somewhat higher than the typical values of 0.05 to 0.2 nm/s for CuPc layer deposition for OLEDs [13]. The layers were grown at substrate temperatures of $T_s = 23$ (sample 1) and 50°C (sample 2), respectively. Under these growth conditions the film is expected to be in the α form (see for instance Refs. [14–16]), which is monoclinic [16] (nearly tetragonal, $\Theta = 90.4°$). The average thickness of the CuPc films, measured as explained below, was approximately 10 nm. Measurements were also performed on sample 2 after annealing at 320°C for 1 h. This temperature is well above $T_\beta = 207$°C, where the transition into the β polymorphic form (monoclinic, $\Theta = 120.56°$), takes place in bulk material [16]. The STM spectroscopy measurements were performed by ramping the tip bias voltage, V_T, while the STM feedback electronics maintains a constant current. In this way, tip-height vs. V_T curves (z-V curves) were obtained. For a more detailed description of the technique, see [17,18]. In this study the z-V curves were obtained during the collection of an STM image by pausing the tip scanning motion for the time necessary to collect data at selected spots of the image window. The CuPc film is not dramatically disturbed by the tip penetration of the organic layer: rather it shows self-healing properties. All the z-V curves presented in this report are raw data with no correction made for thermal drift or piezo creep in the z direction.

III. RESULTS AND DISCUSSION

A. STM imaging: Polymorphic phases

STM images of the unannealed sample grown at room temperature reveal a rough surface morphology without indications of crystalline order. For this sample the tunneling junction was quite noisy leading to poor imaging conditions. For the annealed sample, however, the CuPc thin film consists of crystallites exhibiting various polymorphic forms, some of which are very similar to the bulk α and β phases and their distribution depends on the thermal treatment of the sample, see below. Best imaging conditions were obtained for a voltage bias of $V_T \sim 1$ V, positive tip polarity, and low tunneling currents, $i_T = 2$ to 30 pA. STM images were collected at voltage biases as high as 3.5 V. For negative tip polarity reasonably good imaging conditions were achieved in the range from 6 to 60 pA and $V_T \sim -0.8$ to -1.3 V. Higher voltage magnitudes or, surprisingly, lower currents led to less stable tunneling conditions. These tunneling parameters should be compared to those reported for STM investigations of isolated molecules and monolayers of CuPc deposited on Au(111) or Ag surfaces, where tunneling currents of several 100 pA up to 7.7 nA are used [10,19–23], whereas the magnitude of V_T is, at most, slightly below 1 V. The STM technique does not damage the molecular species, even when tunneling at such high current densities, and can be used to probe the filled as well as the empty levels. There is evidence, additionally, of a general trend that at low voltage bias, approximately 100 mV, higher tunneling currents can be sustained [10,22]. Regarding our samples the fact that stable tunneling conditions are established at higher tunneling resistances than those typically used for low CuPc coverages can be rationalized in terms of the higher electrical resistance of the thicker CuPc layers.

In the following, we discuss the various polymorphic forms found in our samples by STM. In the case of the as-grown sample 2 the STM images indicate the existence of disordered regions, where no stable tunneling conditions are achieved, interspersed with a small fraction, below 10%, of crystallized regions where stable tunneling can be sustained. The crystallites

are polymorphic with single-phase domains of lateral dimensions smaller than 30 nm. In this sample we can identify three different monoclinic polymorphs, which we denote α_1 (nearly tetragonal), β_1 and γ (nearly hexagonal). After annealing we find that the thin film consists only of crystallites with larger domains, at least 100 nm in lateral extension. Figure 1 shows an STM image of a region of the sample exhibiting various polymorphic phases. We find that most of the domains have transformed into a different monoclinic phase, which we call β_2, whereas the low-density γ phase disappears. Domains of α_1 and β_1 phases, however, subsist after thermal treatment, indicating that full conversion into a single phase was not achieved. Figure 2 shows phase γ observed on the as-grown sample 2 and phases α_1, β_1, and β_2 observed on sample 2 after annealing. An analysis of the STM images reveal that, for all phases reported here, (i) the column of stacked molecules lies, within the experimental error of a few degrees, perpendicular to the surface plane and (ii) the plane of the molecules is perpendicular to the stacking direction. This packing habit has also been found for CuPc thin films deposited on highly oriented pyrolytic graphite (HOPG) [11].

The lattice constants a and c, and the angle θ between the unit vectors of the lattice of the crystalline phases were determined by measuring the intermolecular distances in the images as shown schematically in Fig. 3. The vertical distance between the molecular planes, b, is determined by measuring the step height between terraces of crystallites. The results, shown in Table I, represent the analysis of about 130 different STM images. We find that for the α_1 and β_1 phases the intermolecular distances in the a-c plane are similar to those of the bulk α and β phases, respectively [16,24]. Remarkably, the interplanar distance between the molecules in our thin films is significantly smaller than for the bulk phases, 0.32 nm [25,26]. Hence we find $b = 0.23 \pm 0.01$ to 0.26 ± 0.01 nm, depending on the crystalline phase, see Table I. This is in contrast to $b = 0.33$ nm measured with STM on a CuPc thin film on HOPG by Mizutani et al. [11]. We note that isolated CuPc molecules on a Cu(001) [20] and on HOPG surfaces [9] imaged with STM show an apparent CuPc molecular thickness of 0.2 nm. For GaAs(110) surfaces the apparent thickness CuPc molecules is approx. 0.15 nm [27]. Lu et al. report that the benzene portion of metal phthalocyanines on Au(111) has a height of 0.21 nm [22]. It should be noted, however, that STM imaging of molecules adsorbed for example on a metallic substrate can lead to anomalous heights due to the different density of states between the two materials.

B. STM imaging: Modified herringbone reconstruction

The CuPc-covered Au(111) surfaces show that the herringbone reconstruction typical of the clean metal surface is mimicked on the CuPc surface. Figure 1 shows a typical example. The peak-to-peak corrugation is 0.02-0.025 nm, which is very similar to that measured on the bare substrate, namely 0.02 nm. We find, however, that the periodicity of the reconstruction is $\approx$7.3 nm instead of $\approx$6.3 nm for the clean Au(111). Modifications of the Au(111) reconstruction upon adsorption of molecules [28] or by contact with liquids [29] have been reported previously, and are attributed to changes in surface stress [30]. The increase of the periodicity observed in our samples, $\approx$17%, is much smaller than that observed on C_{60}-covered Au(111) surfaces, $\approx$43 to $\approx$100% [28]. This indicates that the CuPc molecules induce a much smaller change of surface stress than the C_{60} molecules. This can be understood considering the weak in-plane interaction of the molecules in CuPc thin films.

C. STM Spectroscopy

The z-V technique differs from standard STM current-voltage spectroscopy, performed with the feedback loop disabled, where the changes in the tunneling current with voltage are ascribed to the energy dependence of the density of states [31]. In the z-V technique, the density of states as a function of the voltage is also probed, but instead through the change of the tip height. More specifically, as the bias voltage is decreased, at some point the Fermi level of the tip (E_F) moves close to the LUMO (negative tip polarity), or to the HOMO level (positive tip polarity) the tip penetrates the organic layer until at a specific threshold bias-voltage it reaches the CuPc/metal interface. The step threshold, which we determine by linear interpolation, marks the energy level for the onset of charge carrier injection via polaronic states into the organic material (rather than resonant or non-resonant tunneling through a dielectric).

Figures 4a-c show typical z-V spectra for the α_1, β_1, and β_2 phases. For these measurements the bias voltage was ramped with decreasing magnitude for each polarity. Typical z-V curves for a clean Au(111) substrate are shown as dashed lines. The height difference between the two curves in the high-voltage region is an approximate measure of the local thickness of the CuPc thin film. At high bias voltages the molecules at the free surface of the thin film can be clearly imaged, see Fig. 1. As the bias voltage is decreased we observe that the tip moves into the thin film in a step-like fashion, initially by only one or two molecular spacings. In some cases the z-V curves exhibit several step-like transitions, see Fig. 4. Then at a characteristic threshold bias voltage the tip penetrates the thin film abruptly until it reaches the CuPc/metal interface. Our measurements show that at this point charge carriers can be injected either from the tip directly into the substrate or via nonresonant tunneling through CuPc molecules in contact with the substrate. Thus we find that after penetration of the thin film, images of molecules can be obtained even at bias voltages as low as 50 meV, in agreement with reports by other researchers [20,21]. When the bias is further reduced to about 20 meV, at $i_T = 10$ pA, the interfacial molecules are forced out of the tunneling junction and then STM images are obtained that clearly show features typical of the clean Au(111) substrate.

From the detailed analysis of a few hundred z-V spectra we deduce the statistical distribution of the single-particle gap $E_{\rm gsp}$, the electron and hole injection threshold energies at the CuPc/Au(111) interface, E_e and E_h respectively, for the different polymorphic phases. We obtained for α_1: $E_{\rm gsp} = 180 \pm 60$ meV, $E_e = 80 \pm 40$ meV, $E_h = -100 \pm 40$ meV; for β_1: $E_{\rm gsp} = 830 \pm 180$ meV, $E_e = 210 \pm 70$ meV, $E_h = -620 \pm 170$ meV; and for β_2: $E_{\rm gsp} = 300 \pm 70$ meV, $E_e = 100 \pm 50$ meV, $E_h = -200 \pm 50$ meV. A striking feature of the spectra for the polymorphic phases of Figs. 4a-c is the high steepness of the curves near threshold, $dz/dV \cong 2 \times 10^2$ nm/V. In comparison, on conjugated polymers, e.g. poly(*p*-phenylenevinylene) (PPV) [32], an alkoxy PPV derivative [17] and small molecules, e.g. *tris*(8-hydroxyquinolato)aluminum (Alq_3) [18], the slope is typically 3-5 nm/V. Actually the z-V curves collected on CuPc resemble the ideal near-step function expected for a highly conducting material [18]: in the high-voltage range the tip follows approximately the z-V curve of the clean metallic substrate until, suddenly, it penetrates the sample deeply when its Fermi level shifts to energies within the forbidden gap. Thus the curves show that the conductivity of CuPc is much higher than that of the other materials studied using this spectroscopic technique. This result is plausible considering that the mobility of CuPc, which is in the range of 10^{-3} cm^2 V^{-1} s^{-1} (cf. e.g. Ref. [33]), is at least one order of magnitude higher than that of the other materials mentioned above. A surprising result is the indication that, for electron injection from the tip, the resistance of the CuPc film appears to be comparable to that for

hole injection. This supports the recent report of Hung and Tang [6], who, using CuPc as part of the cathode structure, conclude that CuPc does not seem to hinder electron transport. We note, however that this result is qualitative because the slope of the threshold of the z-V curves can be influenced by such factors as the potential drop within the organic material and the shape of the injection barrier. The latter is sensitive to the sharpness of the tip. Additionally the charge carrier mobility, μ, of the material is a field-dependent quantity, see Ref. [24].

In the as-grown sample 2 the tunneling junction was much more unstable than after annealing. Still we were able to take a few spectroscopy measurements, but only for positive tip polarity. From these measurements we can deduce $E_h = 170 \pm 70$ meV. This value corresponds most probably to disordered regions of the sample. As mentioned above, the tunneling conditions on sample 1 were somewhat unstable and it was difficult to produce STM images. No indication of molecular order was found for this sample and, as shown below, the charge transport quality is inferior to that of the crystalline phases. In spite of this, we were able to collect quite reproducible z-V curves. Figure 5 shows two examples. For this sample we found the largest values for charge-injection thresholds. Here we obtain $E_e = +550 \pm 150$ meV and $E_h = -550 \pm 150$ meV. From measurements where the voltage is ramped from positive to negative bias in a single sweep, we obtained $E_{\rm gsp} = 950 \pm 100$ meV, see Fig. 5b. The advantage here is that E_e and E_h are determined at exactly the same position on the sample, resulting in smaller fluctuations of the threshold values. Clearly the data indicates a tendency to decrease the charge-carrier injection gap while increasing the degree of crystallinity of the thin films. Note also that the average slope of the z-V is less steep than for the crystallized sample, see Fig. 4. This indicates a lower conductivity for disordered samples. The results are summarized in Table II. It can be seen that for the various polymorphs, E_h is more sensitive than E_e to the crystal structure. On the other hand, considering that the reported values of the ionization potential of CuPc thin films are in the range of 4.7 to 5.3 eV [4,34] and that the work function of the clean Au(111) surface is $\phi = 5.31$ eV [35] we would expect, assuming a common vacuum level (CVL), the HOMO level of CuPc to lie in the energy range $0 \lesssim E_h \lesssim 600$ meV, i.e. just at or above the Fermi level of the substrate. The results in Table II show, however, that for all cases the HOMO level lies clearly below the Fermi level of the substrate. This result shows that the CVL approximation does not hold for the interface between the different CuPc polymorphs and Au(111) and indicates the presence of a dipole layer at the interface and/or the effect of image forces. Additionally, our data clearly shows that the samples characterized by z-V curves with a steep drop at the charge injection threshold (Fig. 4) exhibit a smaller band gap than those where the slope is shallow (Fig. 5). This reflects the influence of the molecular packing on the energy levels and transport properties of the thin films.

For all the polymorphic phases identified in our samples the injection gap is much smaller than the optical absorption threshold measured on CuPc thin films of different polymorphic phases $E_a \cong 1.6$ to 1.7 eV [14,36,37].

We note that a charge injection gap smaller than the optical gap would be expected in the case of electron injection into the $e_g(\pi^*)$ triplet state in the presence of a hole in the $a_{1u}(\pi)$ orbital of a molecule, corresponding to the optically forbidden $S_0 \rightarrow T_1$ transition at 1.15 eV [38]. This coincidental transition, which has been probed with inelastic electron tunneling spectroscopy [39], is however quite improbable and its contribution to the tunnel current is therefore very small. The absorption threshold is assigned to the optically allowed transition $a_{1u}(\pi) \rightarrow e_g(\pi^*)$ by comparing experimental results to theoretical calculations for isolated molecules assuming D_{4h} symmetry. The HOMO level is the $a_{1u}(\pi)$ state, which is composed primarily of p_z orbitals of the nitrogen and carbon pyrrole atoms [40,41]. Concerning the

LUMO level, different theoretical studies disagree on the relative position of the uppermost partially filled Cu d levels with respect to the $e_g(\pi^*)$ state [40–43], and there is even disagreement on the symmetry of the uppermost Cu d level [41]. The consensus seems to be that the partially occupied b_{1g} state, the Cu $(d_{x^2-y^2})$ orbital, is located within a few 100 meV of the $e_g(\pi^*)$ orbital energy [42,43].

Our results cannot be explained in the framework of isolated molecule approximation and indicate its limitations. Consequently for a deeper understanding of the charge-injection and transport phenomena observed it is necessary to take into account the effect of intermolecular interactions on the electronic properties of the material. For instance the small intermolecular distance in the stacking direction, significantly smaller than the van der Waals radius, is an indication of the strength of the interaction. One-dimensional band structure of metal phthalocyanines has been studied by means of a tight-binding method based on the Hückel formalism [44] by discrete variational X-α calculations [40], and by density functional calculations, where the effect of molecular packing has been simulated by considering CuPc as a one-dimensional molecular metal [41]. Those studies show that the energy gap, determined by the $a_{1u}(\pi)$ and the partially filled b_{1g} orbital [40], is very sensitive to the intermolecular interactions in the stacking direction in two ways: (i) a broadening of the ligand-centered molecular orbitals owing to overlap, which gives rise to a dispersion of the energy as a function of the wave vector k in the stacking direction, creating an indirect energy gap, and (ii) a lowering of the energy of the highly localized metal-centered molecular orbitals relative to the ligand molecular orbitals. Thus the effect of stacking results in a reduction of the HOMO-LUMO gap with increasing strength of the intermolecular interaction. In the case of NiPc, for instance, Kutzler et al. [40] predict that stacking effects may reduce the gap to less than one-fourth of the optical band gap, or even cause it to disappear in the case of Ni-tetrabenzoporphyrinato. Basically our results confirm the trends predicted by these theoretical studies and show, additionally, that the packing of the molecules can have a strong influence on the transport properties of the material.

IV. CONCLUSIONS

In summary, we find that the energy gap for charge-carrier injection into thin films of CuPc depends strongly on the intermolecular packing and crystallographic order of the molecules. Our results suggest a tendency of decreasing gap energy and improved charge transport properties with increasing degree of crystalline order in the thin film. We also find that the gap is sensitive to the polymorphic phase of the material. In addition we find indications that some polymorphic phases of CuPc can exhibit good electron transport properties. For the disordered CuPc domains as well as for all the polymorphs reported in this study the single-particle gap measured by z-V spectroscopy is much smaller than the optical band gap measured on thin films. Qualitatively these results agree with theoretical studies where intermolecular interactions in the stacking direction are taken into account. These interactions can induce a strong reduction of the band gap due to a shift of the topmost half-filled Cu d molecular orbital below the $e_g(\pi)$ level and by a broadening of the ligand-centered molecular orbitals.

Regarding the alignment of the energy levels of CuPc with respect to the substrate, we find that the position of the HOMO level lies significantly lower than expected in the CVL approximation, and its energy exhibits a much stronger dependence on the polymorphic phase than the LUMO levels, indicating the formation of a dipole layer and/or the effect of image

forces at the metal-organic interface.

Finally we find an adsorbate-induced modification of the Au(111) surface reconstruction. The change of surface tension induced by the CuPc molecules on the metallic surface is consistent with a weak lateral interaction between CuPc molecules at the metal-organic interface, which tend to form one-dimensional conducting stacks oriented in a direction perpendicular to the surface.

ACKNOWLEDGMENTS

We thank R. Schlittler for invaluable help in setting up the STM used in this study, P. F. Seidler for his enthusiasm and support as well as for fruitful discussions, and W. Andreoni, A. Curioni, and U. Dürig for very fruitful discussions. Thanks also to H. Riel for providing the optical absorption measurements on CuPc thin films.

---

[1] S.A. Van Slyke and C.W. Tang, U.S. Patent 472,043,2 (1988).
[2] C.W. Tang and S.A. Van Slyke, Appl. Phys. Lett. 51, 913 (1987).
[3] C.W. Tang, S.A. Van Slyke, and C.H. Chen, J. Appl. Phys. 65, 3610 (1989).
[4] S.A. Van Slyke, C.H. Chen, and C.W. Tang, Appl. Phys. Lett. 69, 2160 (1996).
[5] G. Pathasarathy, P.E. Burroughs, V. Kahlfin, V.G. Kozolov, and S.R. Forrest, Appl. Phys. Lett. 72, 2138 (1998).
[6] L.S. Hung and C.W. Tang, Appl. Phys. Lett. 74, 3209 (1999).
[7] Z.Q. Gao, W.Y. Lai, T.C. Wong, C.S. Lee, I. Bello, and S.T. Lee, Appl. Phys. Lett. 74, 3269 (1999).
[8] J.K. Gimzewski, J.H. Coombs, R. Möller, and R.R. Schlittler, "Scanning tunneling microscopy of molecular clusters of copper phthalocyanine adsorbed on silver surfaces," in *Molecular Electronics-Science and Technology*, (Engineering Foundation, New York, 1990) p. 87.
[9] C. Dekker, S.J. Tans, B. Oberndorff, R. Meyer, and L.C. Venema, Synthetic Metals, 84, 853 (1997).
[10] X. Lu and K.W. Hipps, J. Phys. Chem. 101, 5391 (1997).
[11] W. Mizutani, M. Shigeno, Y. Sakakibara, K. Kajimura, and M. Ono, J. Vac. Sci. Technol. A8, 675 (1990) and references therein.
[12] J.V. Barth, H. Burne, G. Ertl, and R.J. Behm, Phys. Rev. B 42, 9307 (1990).
[13] H. Riel and T. Beierlein, personal communication.
[14] H. Yoshida, Y. Tokura, and T. Koda, Chem. Phys. Lett. 109, 375 (1986).
[15] K.F. Schoch, J. Greggi, and T.A. Temofonte, J. Vac. Sci. Technol. A6, 155 (1988).
[16] A.W. Snow and W.R. Barger, "Phthalocyanine Films in Chemical Sensors," in *Phthalocyanines Properties and Applications*, C.C. Lenznoff and A.B.P. Lever, eds., (VCH Publishers, New York, Weinheim (Germany), Cambridge (UK), 1989) p. 341.
[17] S.F. Alvarado, P.F. Seidler, D.G. Lidzey, and D.D.C. Bradley, Phys. Rev. Lett. 81, 1082 (1998).
[18] S.F. Alvarado, L. Rossi, P. Müller, P.F. Seidler, and W. Rieß, IBM J. of Res. & Develop. (to be published).
[19] J.K. Gimzewski, E. Stoll, and R.R. Schlittler, Surf. Sci. 181, 267 (1987).
[20] P.H. Lippel, R.J. Wilson, M.D. Miller, Ch. Wöll, and S. Chiang, Phys. Rev. Lett. 62, 171 (1989).

[21] T. Fritz, M. Hara, W. Knoll, and H. Sasabe, Mol. Cryst. 253, 269 (1994).
[22] X. Lu, K.W. Hipps, X.D. Wang, and U. Mazur, J. Amer. Chem. Soc. 118, 7197 (1996).
[23] K.W. Hipps, X. Lu, X.D. Wang, and U. Mazur, J. Phys. Chem. 100, 11207 (1996).
[24] M. Nakamura and H. Tokumoto, Surf. Sci. 398, 143 (1998).
[25] J.C. Buchholz and G.A. Somorjai, J. Chem. Phys. 66, 573 (1977),
[26] J. Simon and J.-J. André, in *Molecular Semiconductors,* J.M. Lehn and Ch.W. Rees, eds., (Springer, Berlin, Heidelberg, New York, Tokyo, 1985).
[27] R. Möller, R. Coenen, A. Esslinger, and B. Koslowski, J. Vac. Sci. Technol. A 8, 659 (1990).
[28] J.K. Gimzewski, S. Modesti, Ch. Gerber, and R.R. Schlittler, Chem. Phys. Lett. 213, 401 (1993).
[29] K.P. Bohnen and D.M. Kolb, Surf. Sci. 407, L629 (1998).
[30] H. Ibach, C.E. Bach, M. Giesen, and A. Grosmann, Surf. Sci. 375, 107 (1997).
[31] See, e.g., R. Feenstra, Phys. Rev. B 50, 4561 (1994); C.J. Chen, in *Introduction to Scanning Tunneling Microscopy,* Oxford Series in Optical and Imaging Sciences, M. Lapp, J.-I. Nishizawa, B.B. Snavely, H. Stark, A.C. Tam, and T. Wilson, eds., (Oxford Univ. Press, New York, 1993).
[32] L. Rossi, S.F. Alvarado, W. Rieß, S. Schrader, D.G. Lidzey, and D.D.C. Bradley, Synthetic Materials, in press.
[33] R.D. Gould, Thin Solid Films 125, 63 (1985), and references therein.
[34] S.T. Lee, Y.M. Wang, X.Y. Hou, and C.W. Tang, Appl. Phys. Lett. 74, 670 (1999); T. Chassé, C.-I. Wu, I.G. Hill, and A. Kahn, J. Appl. Phys. 85, 6589 (1999); A.J. Ikushima, T. Kanno, S. Yosjhida, and A. Maeda, Thin Solid Films 273, 35 (1996); C. Hosokawa, H. Higashi, H. Nakamura, T. Kusumoto, Appl. Phys. Lett. 67, 3853 (1995); C.S. Xian, K. Seki, H. Inokuchi, S. Zurong, and Q. Renyuan, Bull. Chem. Soc. Jpn., 56, 2565 (1983).
[35] H.B. Michaelson, J. Appl. Phys. 48, 4729 (1977).
[36] E.A. Lucia and F.D. Verderame, J. Chem. Phys. 48, 2674 (1968).
[37] B.R. Hollebone and M.J. Stillman, J. Chem. Soc., Faraday Trans., II, 74, 2107 (1978).
[38] P.S. Vincett, E.M. Voigt, and K.E. Rieckoff, J. Chem. Phys. 55, 4131 (1971).
[39] A. Léger, J. Klein, M. Belin, and D. Défourneau, Solid State Comm. 11, 1331 (1972); S. de Cheveigné, J. Klein, A. Léger, M. Belin, and D. Défourneau, Phys. Rev. B 15, 750 (1977); U. Roll, S. Ewert, and H. Lüth, Chem. Phys. Lett. 58, 91 (1978).
[40] F.W. Kutzler and D.E. Ellis, J. Chem. Phys. 84, 1033 (1986).
[41] A. Rosa and E.J. Baerends, Inorg. Chem. 31, 4717 (1992).
[42] A. Henriksson, B. Roos, and M. Sundbom, Theoret. Chim. Acta 27, 303 (1972).
[43] A.M. Schaffer, M. Goutermann, and E.R. Davidson, Theoret. Chim. Acta 30, 9 (1973).
[44] E. Canadell and S. Alvarez, Inorg. Chem. 23, 573 (1984).

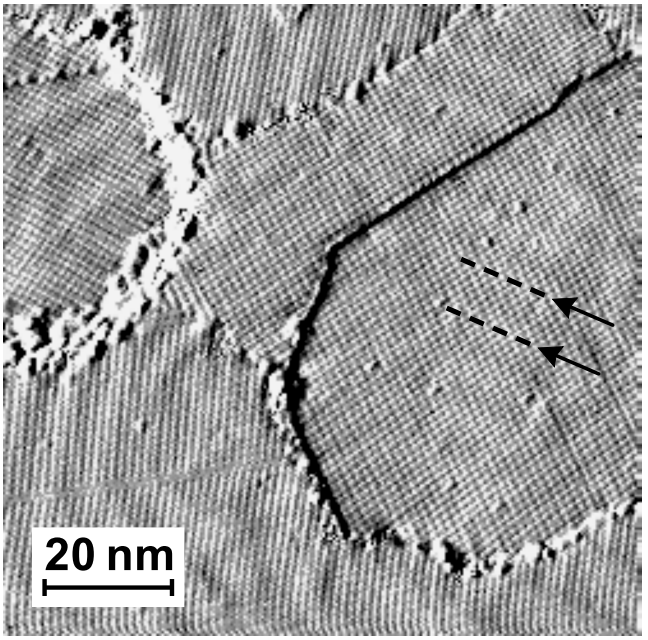

FIG. 1. STM image of the annealed CuPc thin film deposited on a Au(111) substrate. Various domains and polymorphic phases can be clearly seen. The herringbone reconstruction of the underlying substrate is mimicked on the CuPc surface; the arrows indicate its periodicity. Owing to the change of surface stress induced by the adsorbed CuPc molecules, the spacing between rows is 17% larger than for the clean Au(111).

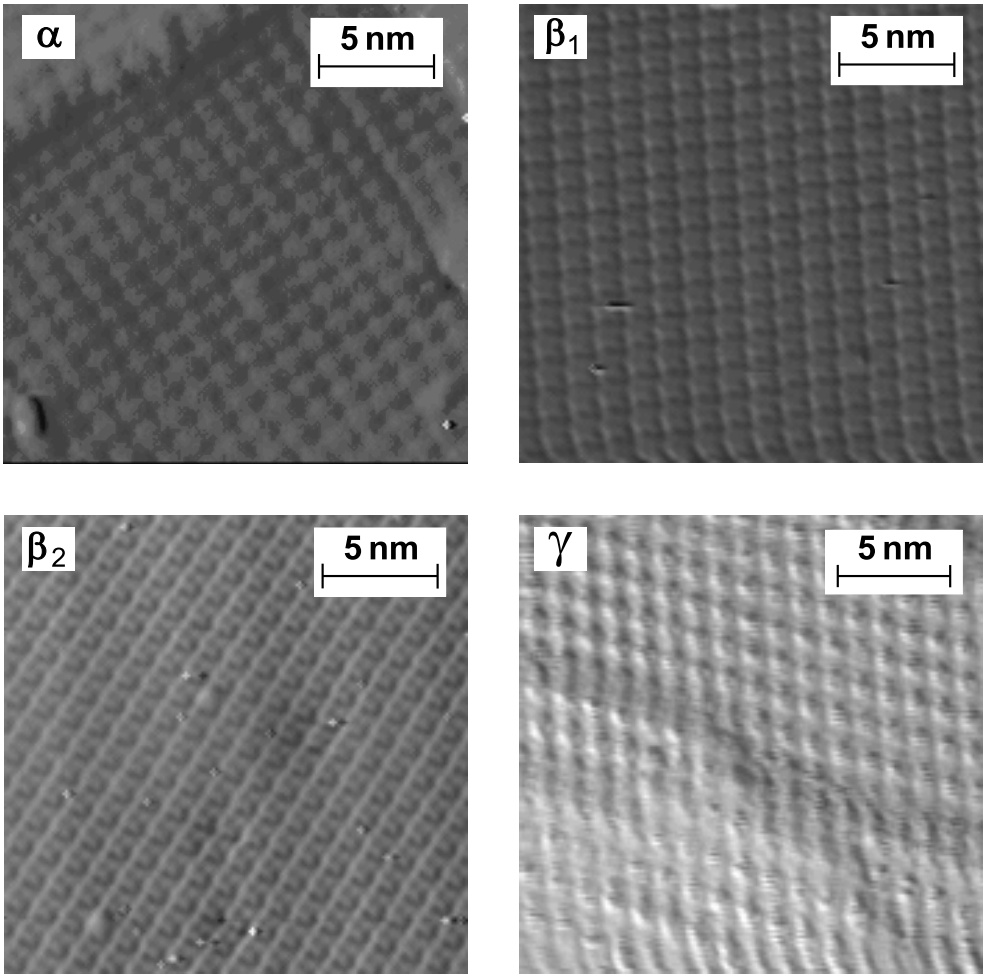

FIG. 2. STM images of the different polymorphic phases found in sample 2 (annealed): α_1 (quasi-tetragonal), tunneling conditions: $i_T = 20$ pA, $V_T = +3.5$ V (positive tip polarity); β_1 (monoclinic), $i_T = 60$ pA, $V_T = -1$ V, β_2 (monoclinic), $i_T = 3$ pA, $V_T = -1$ V; and (as-grown): γ (quasi-hexagonal), $i_T = 2$ pA, $V_T = +0.5$ V. See text for further details.

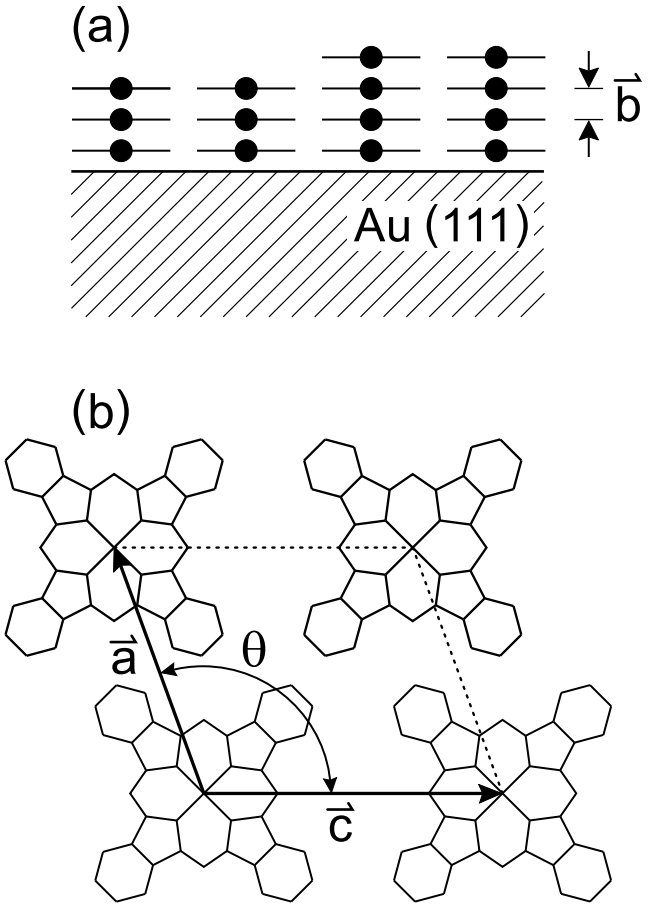

FIG. 3. Scheme of the unit cell parameters used to describe the polymorphic phases of the samples.

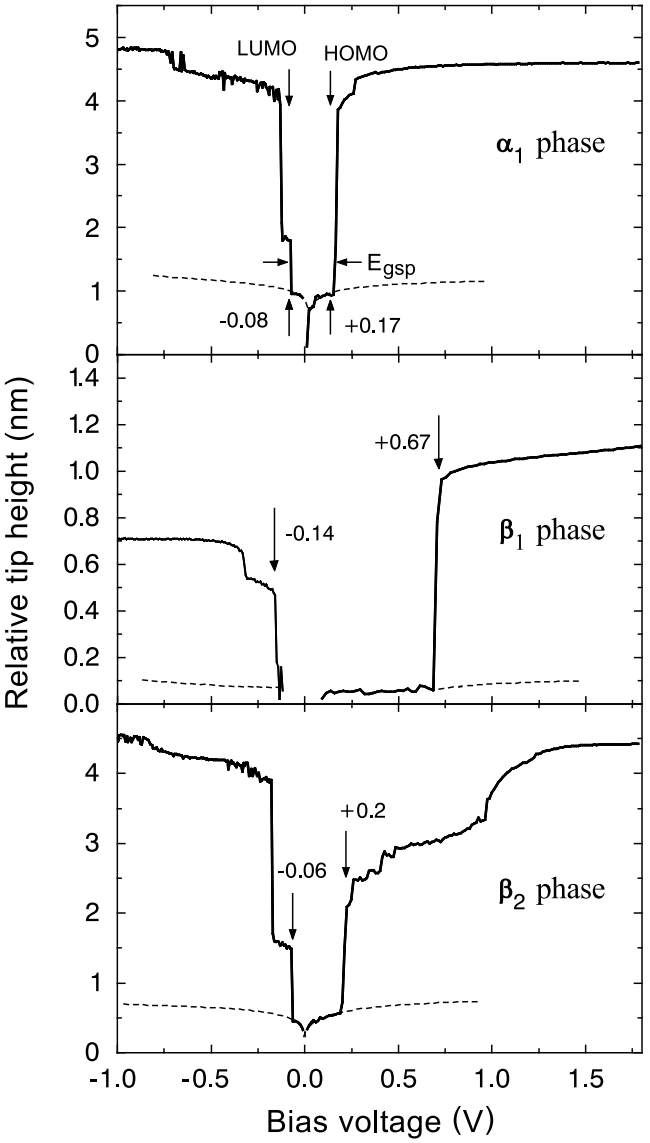

FIG. 4. Typical examples of z-V spectra collected on different polymorphic phases. The dashed lines represent the approximate z-V curve of the bare Au(111) substrate.

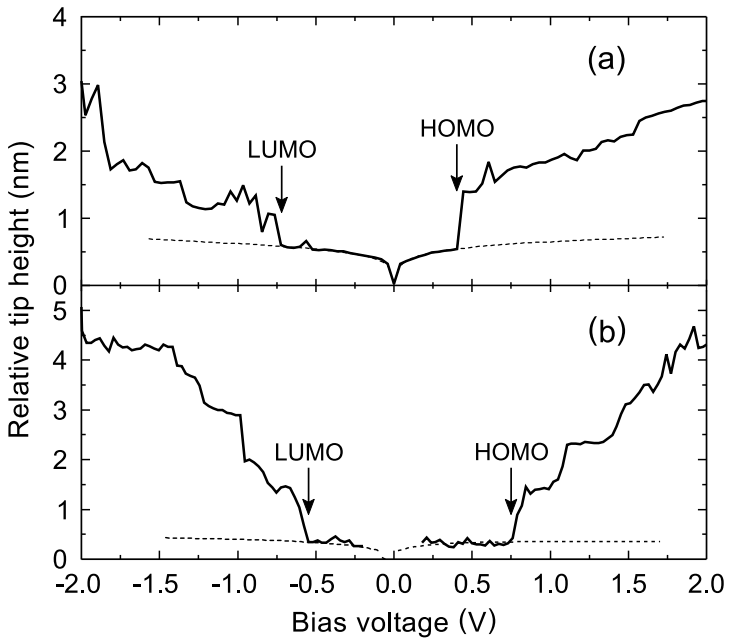

FIG. 5. Examples of z-V spectra collected on regions of the CuPc exhibiting no molecular order, as seen with STM.

TABLE I. Polymorphic phases found in our thin films: α_1 (quasi-tetragonal), β_1 and β_2 (monoclinic), and γ (quasi-hexagonal).

Phase	α_1	β_1	β_2	γ
$\lvert\vec{a}\rvert$ (nm)	1.16 ± 0.03	1.15 ± 0.03	1.23 ± 0.02	1.3 ± 0.13
$\lvert\vec{b}\rvert$ (nm)	0.23 ± 0.01	0.24 ± 0.01	0.25 ± 0.01	0.26 ± 0.01
$\lvert\vec{c}\rvert$ (nm)	1.37 ± 0.04	1.29 ± 0.07	1.32 ± 0.02	1.48 ± 0.1
$\theta = \angle(\vec{a}, \vec{c})$	$91.2 \pm 1.4^\circ$	$94.2 \pm 2.5^\circ$	$100.6 \pm 1.4^\circ$	$111 \pm 1^\circ$
ρ_S (molec./cm^2)	6.33×10^{13}	6.79×10^{13}	6.19×10^{13}	5.21×10^{13}
ρ_V (molec./cm^3)	2.81×10^{21}	2.89×10^{21}	2.53×10^{21}	2.04×10^{21}

TABLE II. Summary of the z-V spectroscopy measurements. E_{gsp} is the energy gap for charge-carrier injection, E_e and E_h are the threshold energies for electron and hole injection into the CuPc thin film, referred to the Fermi energy of the Au(111) substrate. Value marked with an asterisk (*) was measured by ramping V_T from positive to negative bias polarity in a single sweep.

	Sample 1 as-grown $T_S = 23°\mathrm{C}$	Sample 2 as-grown $T_S = 50°\mathrm{C}$	Sample 2 annealed α_1 phase	Sample 2 annealed β_1 phase	Sample 2 annealed β_2 phase
E_e (meV)	550±150		80±40	210±70	100±50
E_h (meV)	−550±150	−170±70	−100±40	−620±170	−200±50
E_{gsp} (meV)	1100±210 (950±100)*		180±60	830±190	300±70